DOI:10.1190/segam2020-3427004.1

Joint Use of Crosswell EM and Seismics for Monitoring CO_2 Storage at the Containment and Monitoring Institute Field Site (CaMI): Baseline Surveys and Preliminary Results

Evan Um, Pierpaolo Marchesini, Michael Wilt, Edward Nichols, David Alumbaugh, Donald Vasco, and Thomas Daley, Lawrence Berkeley National Laboratory; Kerry Key, Columbia University, NY.*

Summary

The goal of carbon capture and geological storage (CSS) is to reduce carbon dioxide (CO_2) release to the atmosphere by capturing CO_2 from powerplants and industrial facilities and subsequently injecting it into a deep permeable geological formation for long-term storage. Successful and safe CCS operations require developing and improving subsurface monitoring technologies for tracking CO_2 movement, evaluating storage integrity and early detection of CO_2 leak from storage. In this study, we present a novel, fully-integrated Electromagnetic (EM) and seismic acquisition system designed to efficiently detect the boundaries of an injected CO_2 plume and monitor its evolution at several stages of injection at a field site. For both methods, we present the preliminary inversion results that will be used as baseline models for future time-lapse crosswell imaging experiments.

Introduction

We introduce a crosswell geophysical system developed at Lawrence Berkeley National Laboratory (LBNL) for imaging a subsurface region between two wells. For this study we employ the system to study the impacts from leakage and secondary accumulation of gas-phase CO_2 at intermediate depths as an analog for a leak into a "thief zone".

Crosswell EM and seismic methods were developed for reservoir monitoring and characterization mainly in oil fields. In these methods, sources are placed in one well and receivers in the other well (Harris et al., 1995; Wilt et al., 1995). As both sources and receivers can be placed in the vicinity of a target, they can sense the target in high resolution compared with surface-based geophysical methods. For imaging a CO_2 plume, we jointly utilize the crosswell EM and seismic. As shown in **Figure** 1, the two methods complement each other and become key to simultaneously monitor and quantify the boundary of a CO_2 plume leakage and plume body saturation. **Figure** 1a indicates that increase in the electrical resistivity directly correlates with the CO_2 saturation. At lower gas saturations the effect is fairly subtle but at higher gas saturation the effect is dramatic (Gasperikova and Hoversten, 2006). Seismic P-wave velocity changes with increasing levels of CO_2 are more complex. There are large changes at low gas saturations and level off at intermediate and higher gas saturations. Although we can see a small continuing change due to density, the P-wave velocity does not appear to have a good correlation with high gas saturation. Thus, the crosswell seismic method is better suited to imaging the boundaries of a CO_2 plume and early detection of CO_2 leakage paths (Vasco et at., 2014). In contrast, the crosswell EM method is better sensitive to the center of the CO_2 plume, reducing uncertainty in seismic rock physics interpretation.

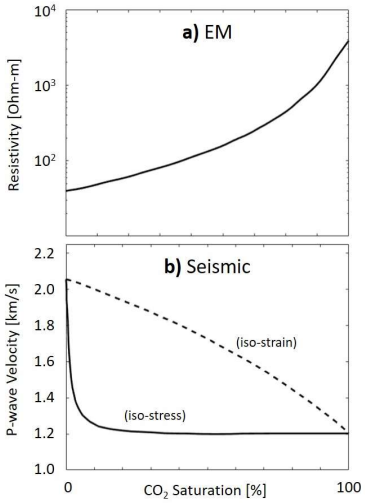

Figure 1. (a) Electrical resistivity as a function of CO_2 saturation *(modified from Gasperikova and Hoversten, 2006);* (b) The lower (Reuss, iso-stress) and upper (Voigt, iso-strain) bounds of P-wave velocity as a function of CO_2 saturation, *(modified from Vasco et al., 2014).*

We present the application of crosswell EM and seismic methods to imaging CO_2 storage at the Containment and Monitoring Institute's Field Research Station (CaMI-FRS) in Brooks, Alberta, Canada. At the site, CO_2 injection is currently ongoing into water-filled sandstones, with overlying shales or mixed sand/shale sequences forming a leaky cap rock (Lawton et al., 2017; Macquet et al., 2019). The remainder of this paper is organized as follows. First, we introduce the Field Research Station, where we assess the crosswell EM and Seismic methods. Second, we describe an integrated EM-Seismic data acquisition system developed at LBNL. Third, we will discuss crosswell EM and seismic baseline data acquisition that occurred in October 2017 before a substantial amount of CO_2 was injected. Finally, we present the baseline crosswell EM and seismic images.

Field Research Station of CaMI

Figure 2 shows the layout of the Field Research Station (FRS) which is located about 200 km east of Calgary, Alberta. A small tonnage of CO_2 (rate of 0.5-1 ton per week) is being injected for a one-year period into a shallow-to-intermediate depth sandstone aquifer at 300 m depth. This site is developed for evaluating and improving new and existing geophysical methods for CCS monitoring purposes

before they are commercially deployed for deep industrial-scale CCS applications.

The FRS has three wells. The central well is a 500 m deep injection well that is directly connected to the CO_2 storage tank on the surface. There are two dedicated observation wells instrumented with various sensors measuring pressure, temperature, strain, seismic, and electric fields. These two observation wells are used for crosswell geophysical methods. Although the wells are drilled vertically deviation logs indicate that the wells are deviated by up to 10 degrees in the injection zone. Accordingly, these logs are used to position sources and receivers in crosswell EM and seismic surveys.

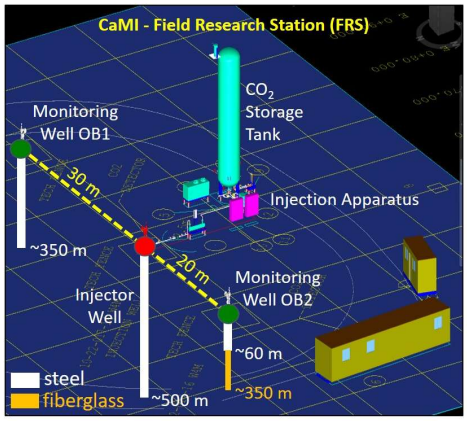

Figure 2. Infrastructures of FRS: Injection Well (in the center) and Observation Wells (OB1 and OB2) are outlined in the three-dimensional framework. The thicker, white lines indicate the steel-cased portion of the wells. In dark yellow, the fiberglass portion of OB2 Well.

Integrated Crosswell EM-Seismic Acquisition System

Figure 3 is a block diagram of the combined crosswell EM and seismic system. The EM system is fully analog where signal is supplied to and received from the borehole antennas using wireline cables. In the next iteration the signal generation and data collection will move downhole.

Except for the antennas most elements of the EM and seismic transmitter systems are the same. Both feature a 7-conductor cable, a high power-high voltage source, a signal generator controlled by a GPS clock and a transformer to capture the current waveform sent to the antenna. Signals are generated using a high-voltage, Insulated-Gate Bipolar Transistor amplifier (IGBT) developed at LBNL. The design of such IGBT unit was designed to overcome durability and performance limitations of off-the-shelf commercial systems.

The EM system terminates in a high-power inductive (coil) transmitter. The 8 cm diameter 4 m length cylinder consists of a laminated transformer steel core wrapped with 500 turns of wire and fully sealed in epoxy. It has an outer fiberglass body with a total weight of 80 kg. Using a current of 10 amps the source has a dipole moment (product of the effective cross-sectional area, number of turns) of 500 A-m^2, sufficient for detection up to 500m away using a frequency up to 1000 Hz. The EM receiver is a 2-level set of axial magnetic coils separated by 5m. The epoxy sealed low noise sensors, allowing them to operate from 10-1000 Hz with a depth range of up to 2 km. Signals are amplified downhole and sent in analog form up the wireline cable.

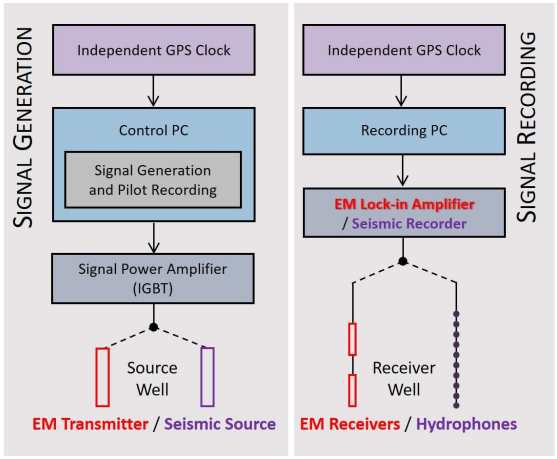

Figure 3. Block diagram of the Integrated EM-Seismic Acquisition System. Two independednt GPS clocks keep the synchronization between the Signal Generation (left) and the Signal Recording (right) sides of the system.

The seismic transmitter is a stack of cylindrical laminated cylindrical piezoelectric ceramic elements (e.g. lead, zirconite and titanite) stacked to make a variable-size source depending on the desired output power. Each element is polarized such that the inner and outer surfaces of the cylinder are positive and negative polarity respectively. When a voltage is applied across the element, it expands or contracts in shape, thus generating a seismic wave when coupled to the earth, typically via fluid in a wellbore.

Data are collected at the surface using a set of lock-in amplifiers synchronized to the source driver (for EM) and a set of digital seismic recorders triggered by driving software (for seismic). Both recording systems effectively stack signals within specified time gates allowing enough acquisition time for unaliased datasets. Both EM and seismic systems operate on the fly. That is, once the receiver array is set within a depth range the data is collected while the transmitter moves. Typically, the EM transmitter moves at the rate of 3-5 m/minute and data are collected every meter, averaging signal within a 20s window. Seismic source is much slower, typically at the rate of 1.2-1.5 m/minute.

Crosswell EM Survey and Inversion

Crosswell EM uses the principles of EM induction to provide an image of the resistivity distribution between wells. An induction coil transmitter is placed in one well and broadcasts sinusoidal EM signals throughout the medium. At the second well, the signals are detected using an array of induction coil receivers. The sources and receivers are normally placed at regularly spaced intervals below, within, and above the depth range of interest and the collected data are used to image the electrical resistivity distribution in the inter-well space.

Crosswell EM works the best in open holes and is also effective if one of the well pairs is steel-cased (Gao et al., 2008). At FRS, Observation well OB1 is steel-cased down to 350 m. Observation well OB2 is fiberglass-cased from 60m to 350m. Although the steel casing severely attenuates EM signals, the effects at frequencies less than a few hundred Hz are fairly moderate and measurements are still effective at imaging the interwell resistivity.

The baseline crosswell EM survey interrogates the interwell resistivity distribution at depths from 200-320 m with one transmitter spaced at 2 m in observation well OB2 and with two receivers spaced at 5 m in observation well OB1. We acquired full tomographic data sets for this well pair at frequencies of 200 and 450 Hz. When the data were pre-processed for inversion, however, we found that the 450 Hz data were too noisy and we used only the 200 Hz data for inversion.

Because observation well OB1 (the receiver well) is steel-cased, the casing effect on the crosswell EM data must be taken care of in the course of inversion or be properly removed before inversion. We choose the latter in this work because this approach is simple and does not require modifying an EM inversion code available to us. First, we extract a common receiver gather from the 200 Hz data. All data points in this gather has the same casing effect. Second, based on well logging data, we construct a fine layered 1D model and simulate the same common receiver gather without steel casing. By comparing the two common receiver gathers, we identify a casing parameter, which is a complex number and explains the attenuation and phase shift of EM fields through steel casing. Finally, the casing parameter is inversely applied to the data. This process removes the casing effect from the data. In general, steel casing properties are not uniform but vary from one receiver position to another. This is the case in observation well OB1. Therefore, we apply this removal process to every common receiver gather and complete the casing-effect-free data.

The final pre-processed data with the top receivers are inverted using the 2.5D finite-element EM modeling and inversion code, MARE2DEM (Key, 2016). For inversion, an individual data point is weighted by the sum of 2% of its own amplitude and 1% of the peak amplitude of a common receiver gather where the data point belongs. **Figure** 4 shows the final crosswell EM inversion. The image shows relatively low resolution because we use only the 200 Hz data and sparse receivers. Overall, the image shows a continuous flat-lying section with a fairly low resistivity contrast. Though the low-frequency crosswell EM inversion cannot recover fine resistivity structures in detail, the interwell image in general agrees well with the logs. This resistivity image will be used as a baseline resistivity model for time-lapse crosswell EM imaging experiments.

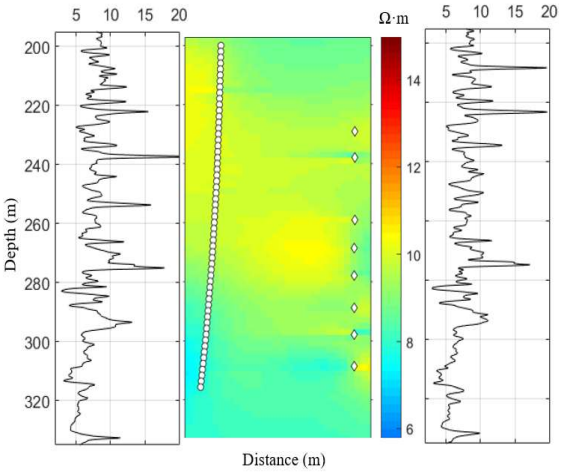

Figure 4. The crosswell EM image with the resistivity logs. An 8 Ohm-m whole space starting model is used. Receiver positions are not uniform as some noisy data are removed.

Crosswell Seismic Survey and Inversion

To complement the EM results, a high-resolution crosswell seismic survey was conducted in the inter-well region of CaMI-FRS to characterize the underlying geology and serve as baseline survey before the (currently ongoing) CO_2 injection started at the FRS site. The survey was carried out using a piezoelectric seismic source that was deployed in the steel-cased, perforated Well OB1. This type of source ensures high signal repeatability, extreme durability (designed for millions of cycles), and guarantees broadband capabilities, from few Hz to kHz (Daley et al., 2007). We raised the source in the well from 344 m to 216 m at 0.5 m depth intervals (257 total source positions). While keeping the source stationary at each depth interval, we generated a series of chirp signals and stacked them into a single record. Every chirp was 200 ms long, 350-2500 Hz in frequency range. The signal was recorded in Well OB2 using a string of broadband hydrophone receivers. The receivers have 5 m spacing for a resulting vertical coverage of 95 m. To match the source shot density (0.5 m), the receivers array required 10 vertical moves, resulting in a total vertical sensor coverage of 99.5 m (0.5 m channel spacing, 200 receiver positions). The whole survey resulted in 257 x 200 = 51400 raypaths and correspondent travel times for tomographic inversion, providing a survey plane from OB1 to OB2,

which crosses the CO_2 injection location at 300 m in the injector well.

An earth model of the CaMI-FRS inter-well subsurface (OB1-OB2) was built based on by linear interpolation from compressional wave velocity logs acquired in OB1 and OB2 (**Figures** 5a and 5d). The earth model served as a framework for inversion (using traveltime picks) based on the current seismic baseline dataset.

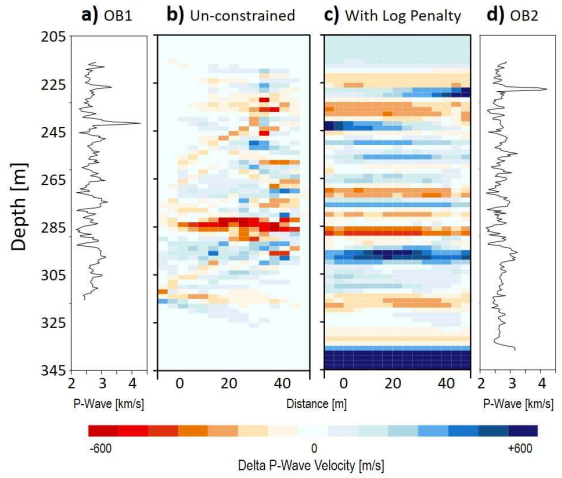

Figure 5. (a), (d) Velocity logs acquired in Observation Wells OB1 and OB2; (b) Un-constrained inversion results based only on first arrival time picks; (c) Constrained inversion results based on earth model (i.e. with log penalty factor).

We produced preliminary inversion results based on P-wave first arrival times and the earth model using a trajectory-based approach (Vasco et al., 1996) for tomographic imaging in an anisotropic medium (**Figures** 5b and 5c). Variations in velocity are within +/-600 meters/sec, with the larger velocity variations observed in correspondence of the injection zone (~290-300 m depth) and in (relatively) superficial areas (above 240 m depth), which could be attributed to the presence of coal lenses in the otherwise silty sandstone subsurface. The larger velocity variation is observed slightly above the injection interval at ~285-290 m depth. **Figure** 5b illustrates the un-constrained result only based on the traveltime picks of the baseline dataset. The tomographic inversion algorithm was tested also with regularization to match well velocity logs (log penalty factor). The use of the subsurface earth to constrain the inversion results, leads to a much more layered inversion (**Figure** 5c).

The quality control evaluation on the applied algorithm shows that many raypaths bend sharply into high-velocity layers (**Figure** 6a), the comparison between calculated and observed first arrival times for P-waves agrees well (**Figure** 6b), and the data misfit illustrates a convergent behavior of the Eikonal solver towards optimal results through a set of five iterations (**Figure** 6c). The QC/QI underlines the importance of studying the changes in the raypaths due to the observed layering of the subsurface. The preliminary inversion based on the current seismic baseline datasets shows a good match between calculated and modeled P-wave first arrival times over the course of several inversion iterations.

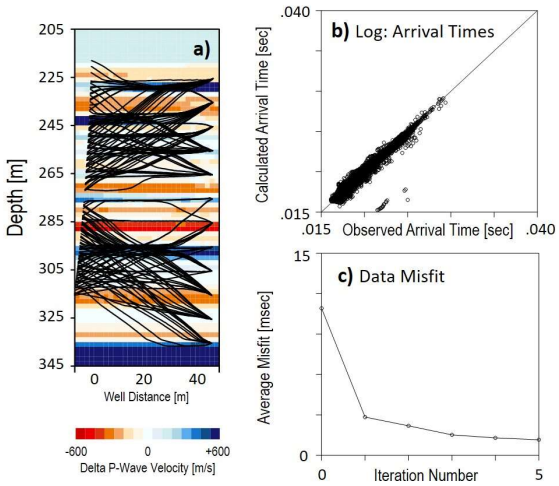

Figure 6. (a) Iterative log of the raypaths during inversion. (b) Calculated vs. observed first arrival times for P-waves in the baseline dataset. (c) History of data misfit (msec)

Conclusions and the Next Step

We have presented a novel, fully-integrated EM and seismic acquisition system designed to monitor the injected CO_2 plume at a CCS research field site. Preliminary results of the inversion of the two baseline datasets show good correlation with resistivity and acoustic velocity logs. These results will be used as baseline models for future time-lapse crosswell imaging experiments after a substantial amount of CO_2 will be injected into the subsurface, allowing for plume detection and monitoring, and for considerations on the impacts of leakage and secondary accumulation of gas-phase CO_2 at intermediate depths as an analog for a leak into a "thief zone".

The first time-lapse set of crosswell measurements is scheduled for late 2020, when more than 30 tons of CO_2 will reside in the space between the observation wells or the overlying stratum. These data along with pressure and flow measurements will be used to map the CO_2 plume, estimate saturations and characterize the leakage environment.

Acknowledgements

We thank Don Lawton, the CaMI Consortium, and all their partners for site access and the help received during field activities. This research was supported by U. S. Department of Energy, National Energy Technology Laboratory, CCSMR program, under the U.S. DOE Contract No. DE-AC02-05CH11231.

REFERENCES

Daley, T. M., R. D. Solbau, J. B. Ajo-Franklin, and S. M. Benson, 2007, Continuous active-source seismic monitoring of CO_2 injection in a brine aquifer: Geophysics, **72**, no. 5, A57–A61, doi: https://doi.org/10.1190/1.2754716.

Gao, G., D. L. Alumbaugh, P. Zhang, J. Liu, H. Zhang, C. Levesque, R. Rosthal, A. Abubakar, and T. Habashy, 2008, Practical implications of nonlinear inversion for cross-well electromagnetic data collected in cased-wells: 78th Annual International Meeting, SEG, Expanded Abstracts, 301–303, doi: https://doi.org/10.1190/1.3054809.

Gasperikova, E., and G. M. Hoversten, 2006, A feasibility study of nonseismic geophysical methods for monitoring geologic CO_2 sequestration: The Leading Edge, **25**, 1282–1288, doi: https://doi.org/10.1190/1.2360621.

Harris, J., R. N. Hoeksema, R. Langan, M. Van Schaack, S. Lazaratos, and J. Rector, 1995, High resolution crosswell imaging of a west Texas carbonate reservoir — Part 1: Project summary and interpretation: Geophysics, **60**, 667–681, doi: https://doi.org/10.1190/1.1443806.

Key, K., 2016, MARE2DEM: A 2-D inversion code for controlled-source electromagnetic and magnetotelluric data: Geophysical Journal International, **207**, 571–588, doi: https://doi.org/10.1093/gji/ggw290.

Lawton, D., K. Osadetz, and A. Saeedfar, 2017, Monitoring technology innovation at the CaMI field research station: Geoconventions.

Macquet, M., D. Lawton, A. Saeedfar, and K. Osadetz, 2019, A feasibility study for detection thresholds of CO_2 at shallow depths at the CaMI field research station, Newell County, Alberta, Canada: Petroleum Geoscience, **25**, 509–518, doi: https://doi.org/10.1144/petgeo2018-135.

Vasco, D., T. M. Daley, and A. Bakulin, 2014, Utilizing the onset of time-lapse changes: A robust basis for reservoir monitoring and characterization: Geophysical Journal International, **197**, 542–556, doi: https://doi.org/10.1093/gji/ggt526.

Vasco, D., J. E. Peterson, and E. Majer, 1996, A simultaneous inversion of seismic traveltimes and amplitudes for velocity and attenuation: Geophysics, **61**, 1738–1757, doi: https://doi.org/10.1190/1.1444091.

Wilt, M. J., D. L. Alumbaugh, H. F. Morrison, A. Becker, K. H. Lee, and M. D. Pan, 1995, Crosswell electromagnetic tomography: System design considerations and field results: Geophysics, **60**, 871–885, doi: https://doi.org/10.1190/1.1443823.